Water Supply

IWA PUBLISHING

Water Supply Vol 23 No 5, 2014 doi: 10.2166/ws.2023.105

Unmanned aerial vehicles for planning rooftop rainwater harvesting systems: a case study from Gurgaon, India

Harish Puppala[a,†], Pranav R. T. Peddinti[b,c,†], Byungmin Kim[b,*] and Manoj Kumar Arora[a]

[a] Department of Civil Engineering, SRM University, Amaravati, Guntur, Andhra Pradesh, 522502, India
[b] Department of Urban and Environmental Engineering, Ulsan National Institute of Science and Technology (UNIST), UNIST-gil 50, Ulju-gun, Ulsan 44919, Republic of Korea
[c] Department of Civil Engineering, Pandit Deendayal Energy University, Raisan, Gujarat 382007, India
*Corresponding author. E-mail: byungmin.kim@unist.ac.kr
[†]Both authors contributed equally.

PRTP, 0000-0002-7397-4899

ABSTRACT

Rooftop rainwater harvesting systems (RRWHS) effectively provide water access by storing precipitated water. The amount of water harvestable using these systems is proportional to the availability of rooftop areas in the region. The use of satellite imagery has gained traction in recent times considering the challenges in conducting a manual survey to determine the rooftop area. However, the limitations on spatial resolution impaired stakeholders from conducting similar assessments in areas with small residential units. In this regard, the use of unmanned aerial vehicles (UAVs) providing high-resolution spatial imagery for the delineation of rooftops of all scales has become popular. The present study is an attempt to utilize UAV-generated orthomosaics to estimate the harvestable quantity of rainwater for setting up an RRWHS. A study area in the Gurgaon district, India, is selected, and the steps involved in estimating the quantity of water harvestable using UAVs are demonstrated. In addition to these computations, a suitable site for constructing the storage unit is identified with the aid of a weighted overlay technique implemented using a Geographic Information System. The results from the study show that nearly 11,229 m^3 of water can be harvested per year in the study site using the RRWHS.

Key words: orthomosaic, rooftop rainwater harvesting system (RRWHS), unmanned aerial vehicle (UAV)

HIGHLIGHTS

- An efficient contactless image acquisition framework for rooftop rainwater harvesting systems was proposed.
- Effective utilization of UAV-generated images for rooftop area evaluation was demonstrated using the Structure-from-Motion technique.
- A multi-criteria decision-making strategy for site selection of the rainwater harvesting system was developed.
- Challenges associated with unsupervised classification for rooftop area delineation in rainwater harvesting were demonstrated.

GRAPHICAL ABSTRACT

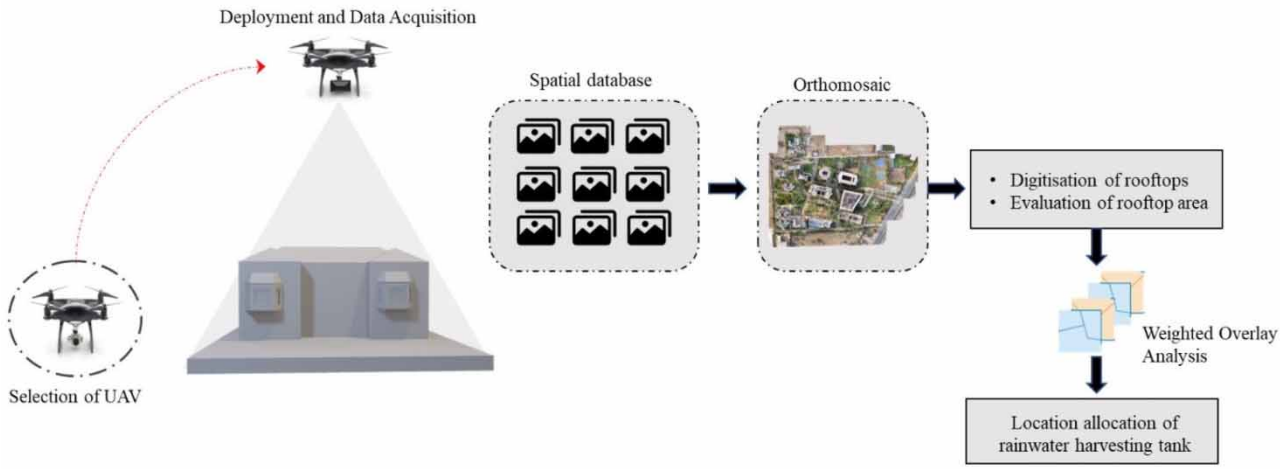

INTRODUCTION

Improved water supply and better water resource management enhance the economic growth of a nation. This, in turn, can alleviate poverty. However, this is completely undervalued globally. Societal pressures with regard to access to water resources have been increasing over the decades. These have become relatively higher due to the increasing population, transient variations in demographics, urbanization, and climate change (Kakoulas *et al.* 2022). Figure 1 depicts the spatial variation in the level of water stress as compiled from the database of the Food and Agriculture Organization of the United Nations (FAO 2022). It is evident that a few nations are experiencing high levels of water stress. Asian countries experience a relatively higher level of water stress than Western counties. The severity is higher in countries such as Algeria, Oman, United Arab Emirates, Egypt, Sudan, Libya, Saudi Arabia, Pakistan, Turkmenistan, and Uzbekistan. This exceptionally high stress has impelled researchers to focus on developing various sustainable solutions that aid community residents to address the problem of inadequate access to water resources (Aguiar *et al.* 2018).

Rooftop rainwater harvesting systems (RRWHSs) constitute one of the effective solutions for providing access to water even in regions experiencing scarcity (Che-Ani *et al.* 2009; Sharma & Begbie 2015) and thereby, ensuring water security. These systems have been in use for a substantial amount of time. In ancient times, the water derived from these systems was used for domestic and agricultural purposes (Angelakis & Koutsoyiannis 2003). In the beginning, cisterns (Angelakis & Spyridakis 1996) were used to store water. The design of RRWHSs progressed over the years with the evolution of hydraulic engineering. The practice of installing rainwater harvesting systems (RWHSs) at a domestic scale in all urban areas is being adopted in various nations (Radonic 2019). Initiatives and strategies undertaken by the governments considering climate change have been supporting the use of the RWHS in recent times as can be seen from the literature (Pala *et al.* 2021; Kakoulas *et al.* 2022). These systems are also considered an intrinsic element of stormwater management techniques (Ward *et al.* 2010). Stakeholders generally adopt the rule-of-thumb principles while designing RWHSs.

However, a systematic design of these systems helps reduce installation, operation, and maintenance costs (Ward *et al.* 2012). In the context of India, a standard design procedure (IS 15797 2008) has been proposed by the Central Public Works Department, Government of India, in their rainwater harvesting and conservation manual (CPWD 2002). In this design procedure, the required volume of the storage tank is estimated by considering the available rooftop area and the average precipitation received in the study area. Various runoff coefficients depending on the type of rooftop have been proposed to account for the losses. The total volume of water that can be collected using an installed RWHS can be computed using the following equation:

$$Q = A \times P \times C_1 \times C_2 \quad (1)$$

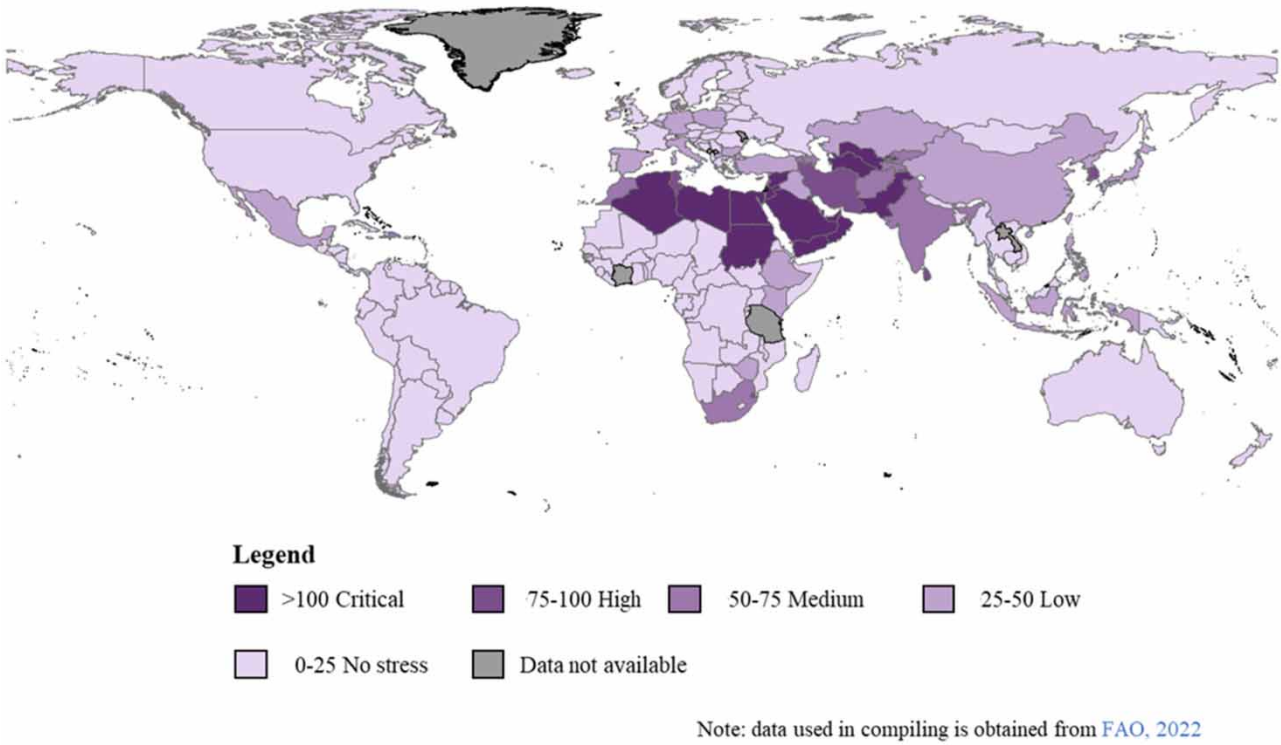

Figure 1 | Classification of countries based on the level of water stress as per Food and Agricultural Organization of the United Nations.

where Q is the effectively harvested water quantity (m^3); A is the rainwater endowment area/rooftop area (m^2); P is the average annual rainfall (m); C_1 is the constant coefficient for the roof surface; C_2 is the constant coefficient accounting for evaporation, spillage, and first flush.

It is apparent from Equation (1) that the rooftop area and roof surface material influence the efficiency of an RWHS. The determination of the rooftop area by conducting a field survey is fraught with measurement errors and is also resource intensive. The restricted access to rooftops could also be a challenge in determining the rooftop rainwater harvesting potential of a community (Shao *et al.* 2021). Considering this, the acquisition of the required information on rooftops using advanced remote sensing techniques has gained traction (Grajfoner *et al.* 2017). The rooftop area of a building has been estimated to the desired accuracy using Worldview-2 data available at a resolution of 2 m in the multi-spectral band and 0.5 m in the panchromatic band (Grunwald *et al.* 2017). These attributes are also estimated at spatial resolutions of 5.8 and 2.1 m using the ZY-3 satellite (Zhou *et al.* 2019). Orthophoto maps generated at a resolution of 0.5 m by the local government of Hong Kong (Tian & Jim 2011), Google map imagery at a resolution of 0.59 m (Huang *et al.* 2015), and aerial imagery at a resolution of 0.4 m (Karteris *et al.* 2016) have also been used to compute the available rooftop area.

Although conventional satellite imagery helps determine the rooftop areas of buildings, spatial resolution is a key barrier. This is particularly so while analyzing the area of small residential units (e.g., with areas $<10\ m^2$). Furthermore, satellite images occasionally do not provide an orthogonal view of the built infrastructure. For example, the image shown in Figure 2(a) does not represent a nadir view of the building. The computation of the area from this would be erratic. This was observed in the case of several buildings irrespective of the number of floors. Occasionally, the rooftops cannot be differentiated from the open-to-air spaces at various levels in the built infrastructure even in the orthogonal view. The area highlighted in Figure 2(b) is not a part of the rooftop. In such a case, the rooftop area computed may be misinterpreted.

Meanwhile, the identification of the type of rooftop material which is essential for selecting the constants in Equation (1) would also be a barrier in the case of coarse spatial resolution imagery. As shown in Figure 2(c), the visual appearance and ground truth of the rooftop material may differ significantly due to the resolution issues in the satellite imagery. Although the rooftop appears to be concrete, it is a corrugated metal roof. These factors influence the assessment of rainwater harvesting capacity. Due to these limitations, Zhou *et al.* (2019) omitted buildings with rooftop areas smaller than 100 m^2 extracted from

Figure 2 | Satellite imagery showing (a) tilted view of buildings in satellite imagery; (b) features that are not a part of building roof; and (c) appearance of corrugated metal roof in satellite imagery.

satellite imagery. This consideration is highly impractical for RWHS studies because an area of 100 m^2 can receive considerable rainfall and contribute a significant quantity of water. A few of the challenges associated with satellite imagery can be overcome using manned aircraft equipped with various sensors. However, aircraft cannot be rapidly deployed at the site due to air traffic restrictions and requires dedicated landing pads/air strips for landing and takeoff operations. In addition, efficient maneuvering of the aircraft requires skilled pilots, thereby increasing human intervention. Furthermore, flying the aircraft is associated with huge operational costs, fuel consumption, and CO_2 emissions.

To mitigate the aforementioned problems, the present study aims to precisely determine the effectively harvested water quantity by appropriate rooftop area assessment and rooftop material identification. In this regard, the use of an unmanned aerial vehicle (UAV) coupled with photogrammetric principles would enable accurate measurement of rooftop areas, which consequently improves the accuracy of conventional RRWHS design. Data collection using UAVs is cost-effective, has a lower environmental impact, and can be rapidly deployed with faster data processing and analysis. Drone-based survey methods can capture higher spatial resolution and more accurate data than aircraft-based methods, resulting in more precise and reliable data, especially for complex or irregular terrain. A UAV is used to collect a series of bird's eye view images that are subsequently used to generate a high-resolution orthomosaic of the study area. Such digital orthomosaics were demonstrated to be effective for identifying key critical features for various engineering applications (Peddinti & Kim 2022). Further nadir view imagery can be generated rapidly given the control against wind, stability, and flexibility of UAVs.

In addition, high-resolution images captured from a suitable height enable better identification of the type of rooftop material. The generated orthomosaic was substantially superior in terms of spatial resolution and accuracy compared with the available satellite imagery. A framework for using the UAV-based mosaics to design a new RWHS for a group of buildings is proposed in this study. A university campus located in Gurgaon, India, is considered to demonstrate the proposed framework. The proposed methodology can be adapted straightforwardly to various built infrastructures ranging from the individual building level to the community level in both rural and urban scenarios. Given the increased attention in all

countries toward developing community-level rainwater harvesting facilities, the present study is likely to improve the accuracy of conventional RWHS methods while saving time and effort.

DESCRIPTION OF THE STUDY AREA

The site selected for this study is BML Munjal University located in Gurgaon district, Haryana, India. Gurgaon district is in the south-eastern part of Haryana state. It has an aerial spread of 1,258 km^2 and a population of approximately 1.51 million. This region experiences a tropical steppe (semi-arid and hot) climate with extreme dry air except in the monsoon months. The moist air of oceanic origin permeates the district causing high humidity, cloudiness, and monsoon rainfall. This district receives an average annual rainfall of 596 mm spread over 28 days (CGWB 2021). The rationale for selecting this area is that the groundwater levels in this district are receding significantly. The primary source of water supply in the region is groundwater, with nearly 93 m^3/day of water being withdrawn from the tube wells (CGWB 2021). The groundwater-cell records show that the groundwater table reduced from 6.64 m in 1974 to 36.99 m in 2021. It was established that the groundwater extraction rate in this district is three times higher than the recharging rate (CGWB 2021). It is apparent that groundwater availability would be a key concern in the near future if this scenario persists. In this regard, the local government administration is inducing the inhabitants to install RRWHSs to reduce their dependency on groundwater. Figure 3 shows the location and a bird's-eye view of the university. Its built infrastructure comprises buildings with numbers of floors ranging between 4 and 13 and various materials used for the rooftops.

METHODOLOGY

A schematic illustration of the framework proposed in this study is presented in Figure 4. The study starts with air space research. Herein, the potential challenges for drone deployment are identified, e.g., birds' movement, tall buildings, trees, and climatic conditions. The flight planning is performed considering the difficulties identified and the aerial extent of the site. Herein, the operating parameters such as the height of flight and speed are determined in accordance with the local UAV laws and regulations.

Figure 3 | Study area selected to determine the rainwater harvesting potential.

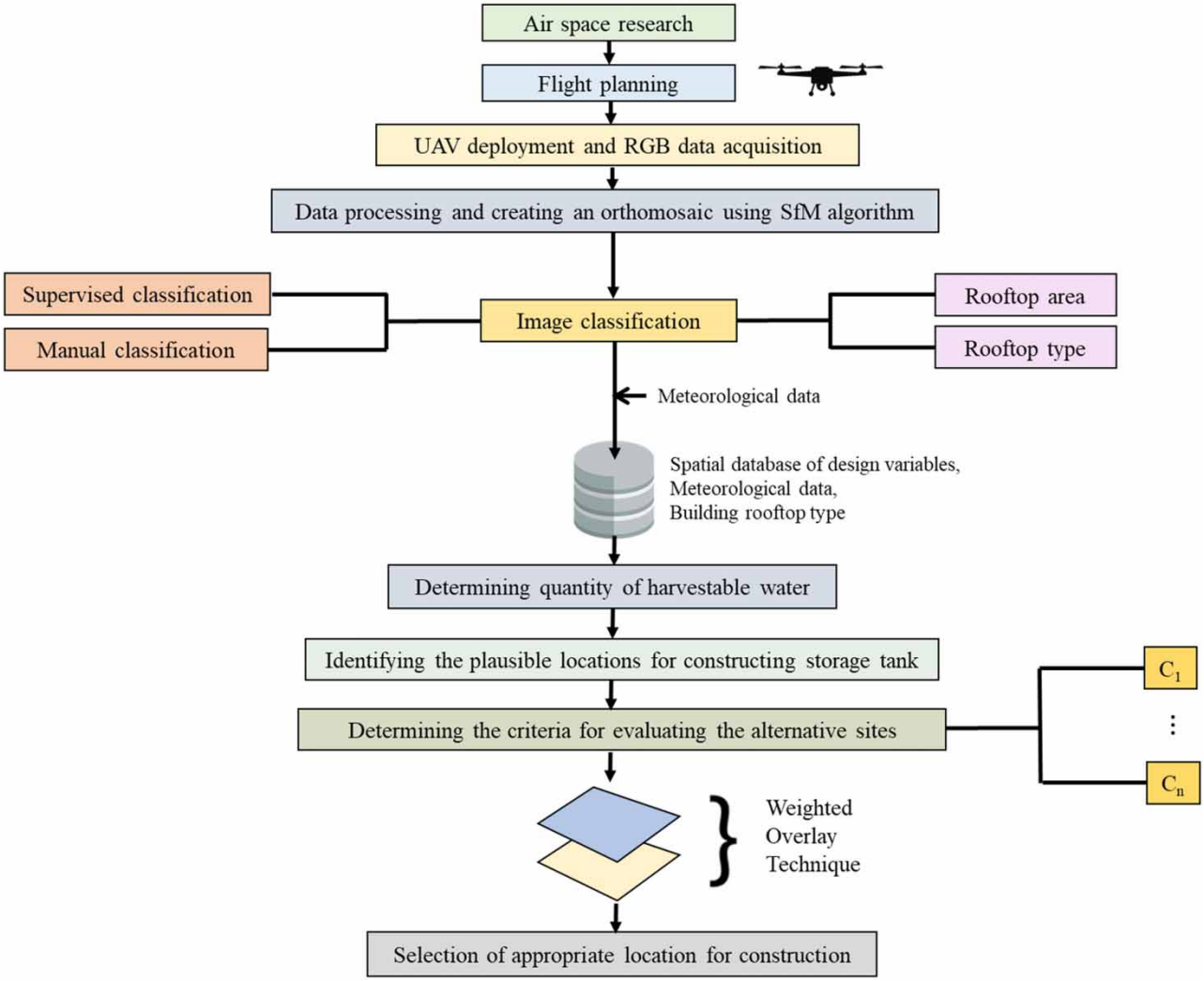

Figure 4 | Schematic illustration of the steps involved in planning a RWHS. (RGB, red, green, blue; SfM, Structure-from-Motion)

Subsequently, the drone is deployed to acquire RGB (red, green, blue) images with the nadir view. After acquiring a series of RGB images, the Structure-from-Motion (SfM) algorithm is used to stitch all the individual images and generate a high-resolution orthomosaic of the study area. The generated orthomosaic provides a synoptic view of the study site. The boundary of each building is delineated using ArcGIS/ArcMap® software. Alternatively, these boundaries can be obtained using either supervised classification or manual digitization techniques. The classified images help determine the rooftop area of each building. Simultaneously, the type of rooftop is determined by inspection. This enables the determination of the coefficient based on the roof surface. The attributes thus computed help determine the volume of the RWHS storage tank. After determining the required storage volume, the feasible location for the storage tank construction is identified by analyzing all the feasible sites. The mathematical aspects of the weighted overlay technique (WOT) (Melese & Belay 2022) are integrated as a part of the proposed framework to conduct the site suitability study. This study proposes two criteria: (i) site suitability score and (ii) installation cost of RWHS calculated using WOT. The site suitability score indicates the likelihood that a given land parcel would be a part of future expansion. Recreational sites such as gardens and playgrounds are eliminated from the site selection analysis. The suitability of each alternative location can be determined in terms of an overall score through this exercise. This score can subsequently be used to determine the most suitable location for the RWHS storage tank. The proposed framework is explained in the following sections based on a pilot study conducted at BML Munjal University.

ANALYSIS AND RESULTS

The university map was initially divided into grids and landmarks to conduct the pilot study. Air space research was performed before the drone flight was planned. The flight path and height were selected to circumvent potential obstructions including towers, birds, and trees, while abiding by the drone flight regulations prescribed by the Ministry of Civil Aviation and Directorate General of Civil Aviation, India. After the preliminary examinations, an aerial survey was conducted using DJI Mavic air 2, a quadcopter with an endurance time of 34 min. The deployed drone has a 48 megapixel RGB camera as a payload. It enabled the drone to collect true color aerial images of the study site.

A total of 1,107 geotagged aerial images were acquired during the survey. The ground sight distance obtained was approximately 2.86 cm/pixel. Ground control points were also established (see Figure 5(a)) to calibrate the geotagged imagery. Subsequently, the professional photogrammetry and drone mapping software Pix4D was used to process the collected images by projecting these on the WGS 1984 UTM 43N coordinate referencing system (CRS). A dense point cloud was generated from the acquired images. On average, 27,798 key points were computed per image. Among these, a minimum of 10,548 matched key points were observed between each set of consecutive images.

The geolocation error was observed to be less than 1.5% in all the three directions. The SfM technique was then applied to stitch these 2D points and generate 3D points. A 3D point cloud with an average density of 142 points per cubic meter was generated in this mapping. Overall, the mean reprojection error from the mapping was 0.141 P. These values depict that the developed digital model is calibrated and has sufficient resolution to represent the ground facts. The outputs generated from this analysis include a high-resolution orthomosaic of the entire study area (see Figure 5(b)). The digital and ground truth measurements were compared at different scales to further validate the digital model (see Figure 5(c)). Table 1 shows that the generated digital model represents the actual physical structures at all sizes and scales. Hence, the generated orthomosaic has been used for the analysis.

Delineation of rooftops from orthomosaic

The present study requires the delineation of the roofs for two important aspects: rooftop area assessment and rooftop material identification. Three approaches have been attempted in this study to investigate the feasibility of an accurate delineation of the information class (i.e., building rooftops from the generated orthomosaic): deep learning models, supervised classification, and manual classification. A detailed insight into the feasibility of adopting these techniques is provided in the following subsections.

Figure 5 | Images of (a) selected features for physical measurement; (b) digital orthomosaic of the mapped area; and (c) digital measurements of the selected features on the developed orthomosaic.

Table 1 | Comparison between physical and digital measurements of selected linear features

Nomenclature of the feature (ref.: Figure 5(a) and 5(c))	Physical measurement of the selected linear feature (m)	Digital measurement of the selected linear feature (m)
A	15.82	15.82
B	3.35	3.35
C	2.51	2.50
D	5.68	5.68
E	2.90	2.90

Deep learning models based on convolutional neural networks

Artificial intelligence (AI) applications have progressed significantly over the years. The accuracy of AI-based models has exceeded those attained by human perception in many cases. Machine learning is one of the available engines that use trained information to classify a given input data. Due to their associated capabilities, deep learning models gained traction from the various architectures of machine learning models. Considering the computational effort involved in training the deep learning models and the limitation in annotated datasets in India, two pre-trained models by ESRI were adopted to delineate the rooftops within the study area. The available deep learning models were constructed based on the theory of convolutional neural networks (CNNs). These can be used to perform both object- and pixel-based classification. In this study, object-based classification was performed using ArcGIS Pro 3.0. Two variants of pre-trained deep learning models developed by considering the data obtained in the context of the USA and Australia were used. The outcomes are shown in Figure 6(a) and 6(b), respectively.

It is apparent from Figure 6 that the accuracy of the deep learning models was not satisfactory. A large fraction of rooftops was not detected. Furthermore, other pixels were mistaken as rooftops, which is glaringly evident from Figure 6(b). For instance, paved surfaces and pathways were detected as rooftops, which is deceptive in Figure 6(a) and 6(b).

Supervised classification by training

In this technique, a training sample set is first generated to train the classification model. The generated training samples can be used to perform pixel-wise image classification after ensuring that these are representative of the study site and are statistically separate. This study applied ArcGIS/ArcMap® software to implement the supervised classification algorithm

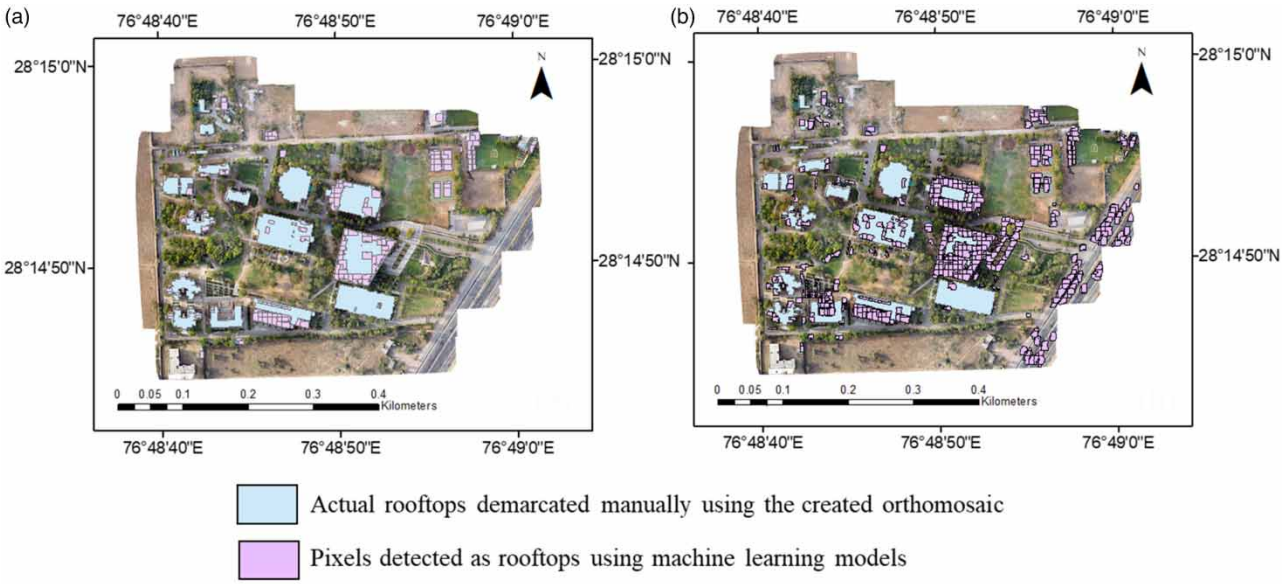

Figure 6 | Delineated rooftops using deep learning models trained using the (a) USA database and (b) Australian database.

using the Image Analysis toolbar. The accuracy of the generated training sample was analyzed using Training Sample Manager in ArcGIS/ArcMap. Although the accuracy of the supervised classification techniques in categorizing the images into different classes is well-established in the literature (Puppala & Singh 2021), its adoption in the context of the current study is inappropriate for several reasons.

For example, the surface at point A lying at the ground level (Figure 7(a)) has texture and color identical to those of the roof of the building shown at point B. The supervised classification algorithm (trained with the sample data of roof) interpreted the surface at point A as roof. This is a mismatch. Figure 7(b) presents the rooftop-installed photovoltaic panels with texture and color different from those of the roofs. Although the rainfall on these roofs would eventually contribute to runoff, the supervised classification tool does not include it in the rooftop category. This results in an underestimation of the rooftop area and quantity of water harvested effectively.

This similarity precludes the use of a supervised classification algorithm. Moreover, for a few of the buildings, the rooftops are installed with cooling towers. These have a color different to that of the rooftops (Figure 7(c)). The generation of training samples by addressing these different materials is resource intensive. Moreover, to detect the type of roof, separate training samples are to be generated for each type. Furthermore, a generalized training dataset cannot be adopted in this case because different construction practices are adopted in different parts of the world. The roof textures, colors (paints), and materials vary significantly across regions. Apart from the aforementioned challenges, although the UAV-based survey helped generate an accurate color orthomosaic, it contains significantly few bands in the visible spectrum. This limitation affects the accuracy of supervised classification (Sibaruddin *et al.* 2018). Over 50% of the rooftop area was indistinguishable from roads when supervised classification is used to delineate the rooftop area in the study of Shao *et al.* 2021. This necessitated substantial user intervention for corrections. Similar problems are reported in the studies by Zhou *et al.* (2019) and Karteris *et al.* (2016).

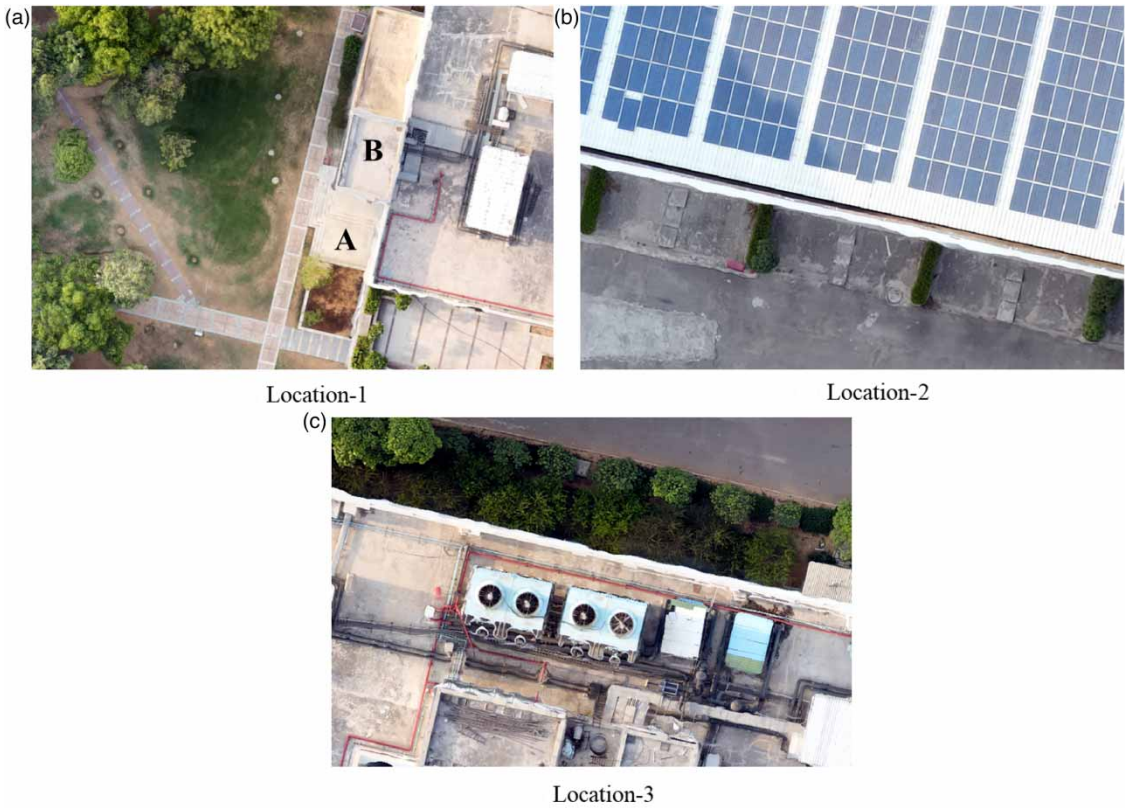

Figure 7 | Images showing the barriers to the adoption of supervised classification to compute rooftop area: (a) no distinction between roof and ground floor; (b) area covered with solar panels is omitted from rooftop; and (c) rooftop area with installed machinery.

Manual classification

This study adopted manual digitization to determine the rooftop area in the study site, considering the aforementioned challenges associated with supervised classification. Furthermore, the rooftops are classified based on the material, which enables the consideration of different constant coefficients for rooftops. This classification is performed via manual digitization. The researchers thoroughly examined the imagery of classified rooftops to prevent potential classification errors. Figure 8 presents the classified rooftops. Here, the concrete and corrugated metal roofs are represented by the identification numbers '1' and '0', respectively (Table 2). The area of each rooftop is calculated using the delineated features (Table 2). Subsequently, the total quantity of rainwater that can be harvested by installing the RWHS is computed as shown in the following.

Effectively harvested water quantity

The total quantity of rainwater that can be harvested by installing the RWHS is determined as follows:

- Total available rooftop area (concrete roof) = 23,412.00 m^2
- Total available rooftop area (corrugated metal roof) = 4,868.88 m^2
- Annual rainfall = 596 mm (0.596 m)
- Constant coefficient for concrete rooftops = 0.85
- Constant coefficient for corrugated metal rooftops = 0.75
- Constant coefficient accounting for evaporation, spillage, and first flush = 0.8

As per Equation (1), the total amount of harvested water quantity is 11.23 million L/year. This requires a storage volume of 11,229 m^3.

SITE ALLOCATION FOR THE RRWHS

The prospective sites for setting up an RRWHS are delineated manually by excluding the playground within the university campus. Figure 9 presents the spatial distribution of alternative sites for constructing the storage tank. It is evident that the installation cost varies with the storage tank location. In addition to the installation cost, it is imperative to consider

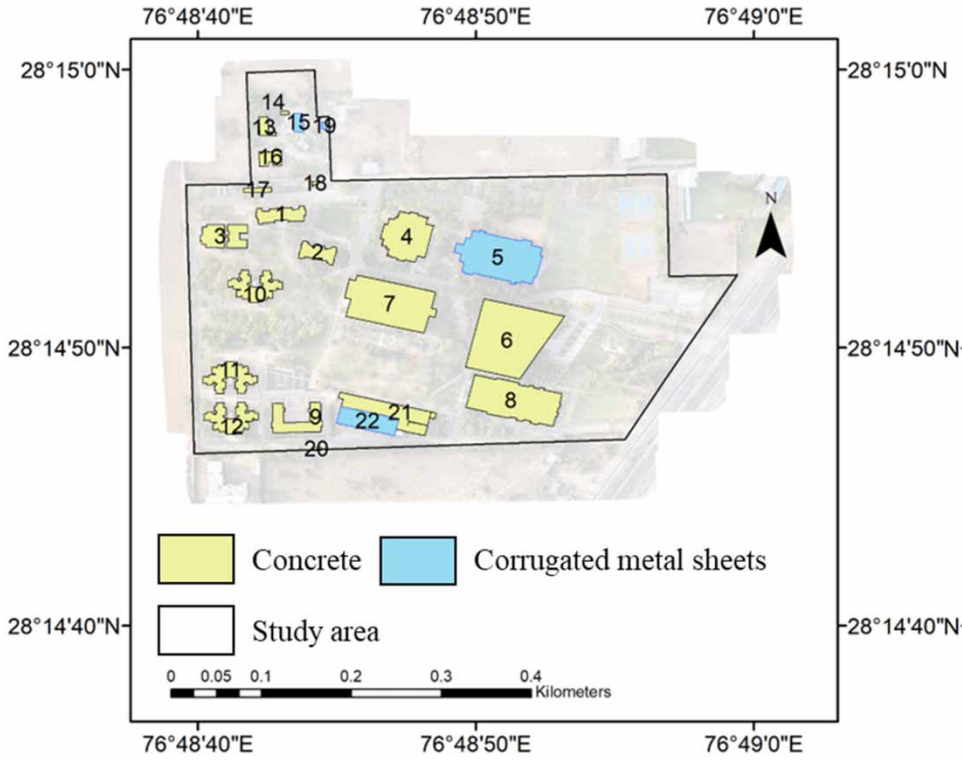

Figure 8 | Delineation and classification of rooftops.

Table 2 | Rooftop area each building within the study site

FID	Building	Rooftop type	Area (m^2)
1	Hostel block-1	1	676.07
2	Hostel block-2	1	562.79
3	Hostel block-3	1	988.48
4	School building-1	1	2,070.02
5	School building-2	0	3,516.65
6	Administrative block	1	5,296.38
7	Faculty block	1	3,892.23
8	Library	1	3,382.41
9	Hostel block-4	1	990.45
10	Hostel block-5	1	1,025.28
11	Hostel block-6	1	1,013.72
12	Hostel block-7	1	1,019.67
13	Staff quarter-1	1	207.64
14	Staff quarter-2	1	34.16
15	Staff quarter-3	0	184.32
16	Staff quarter-4	1	334.26
17	Storeroom-1	1	132.02
18	Storeroom-2	1	24.18
19	Maintenance room	0	41.60
20	Laundry services	1	35.213
21	Workshop building-1	1	1,726.932
22	Workshop building-2	0	1,126.295

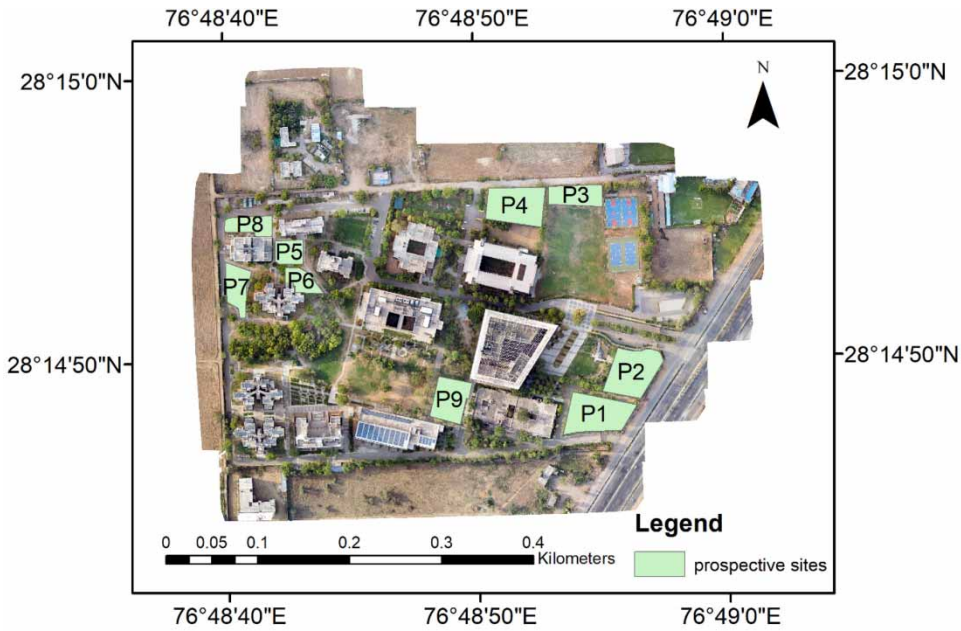

Figure 9 | Prospective sites for storage tank.

the potential extension of the built infrastructure within the university before finalizing the location of the RWHS. Thus, the identification of the appropriate location to install RWHS is a multi-criteria problem. This study adopted the WOT based on Geographical Information System to identify an optimal location for installing the storage tank.

Suitability of the prospective sites

The analysis starts with the identification of available land parcels to construct a storage tank that would collect the water from all the rooftops through a pipe network. Subsequently, an expert panel was constituted. It included the leadership team and the estate management officer. A focused group discussion was conducted with the expert, and a questionnaire was given to each of the experts. The developed questionnaire aims to capture the significance of each alternative site for the prospective construction during the expansion of the built infrastructure of the university. The significance was collected on a scale of 0–5, as shown in Table 3. The existing playgrounds were assigned a score of 0. This represents that the land parcel is excluded from the analysis.

The attributes thus allotted to each land parcel were used subsequently to generate a raster layer showing the variation of the score over the study area (see Figure 10).

Installation cost of the RWHS

In addition to the suitability score, this study considered the installation cost as a criterion affecting the site selection. The distinguishing factors among the prospective sites in terms of installation are the cost of excavation and pipe network. In this study, only the excavation depth (which is proportional to the excavation cost) was considered. This is because it is challenging to determine the length of the pipe network required, without a 3D model of the study area. This model can be constructed only by capturing imagery in different directions. The excavation depth was estimated by considering the available area and the volume of storage required to store the harvestable water estimated using Equation (1). Table 4 presents the estimated field corresponding to a feasible location. These attributes were used to generate a raster and are reclassified to convert the excavation depth into a score ranging between 1 and 5. A score of 5 was assigned to a site with a shallow excavation depth, and the site with a large excavation depth obtained a score of one. The generated raster is shown in Figure 11. The suitability score and excavation score raster (see Figures 10 and 11) were used to perform weighted overlay analysis by assigning scores of 0.7 and 0.3 to the site suitability layer and excavation depth layer, respectively. The resultant raster is shown in Figure 12. It is apparent from the figure that the land parcels lying in the southeast direction are suitable for constructing the storage tank.

DISCUSSION

The performance of the aerial survey using UAV is a simple approach compared to the conventional manual surveys, which require intensive human resources. It is also cost-effective compared with the acquisition of the desired data using high-resolution satellite imagery and aircraft-based surveys. The orthomosaic generated using the imagery obtained using the UAV is a georeferenced image and is devoid of cloud cover. In addition, if the potential for rooftop rainwater harvesting is to be assessed at a community level, permissions to access the rooftops would be challenging. The UAV-based survey could therefore be an optimal solution for community-level assessments. The UAV-generated orthomosaic has a high spatial resolution, typically approximately 1.5–2 cm/P. This enables the monitoring of the thickness of the

Table 3 | The scale developed to rank the prospective land parcels

Suitability level of land parcel for future expansion	Suitability score of expansion	Site suitability for the RWHS
Restricted areas	0	0
Strongly unsuitable	1	5
Unsuitable	2	4
Average	3	3
Suitable	4	2
Strongly suitable	5	1

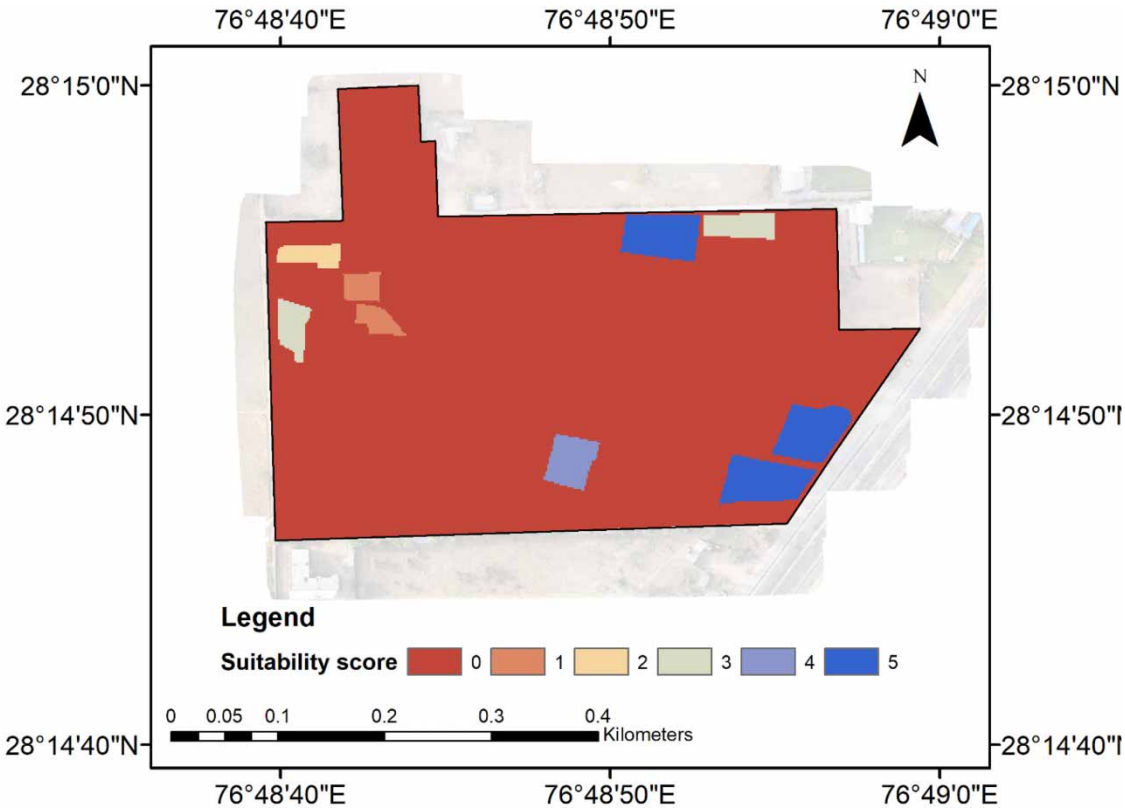

Figure 10 | Spatial variation of suitability score.

Table 4 | Depth of excavation required in each prospective site

Site no.	Site nomenclature	Area (m^2)	Depth of excavation (m)
1	P1	2,517.47	4.46
2	P2	2,450.18	4.58
3	P3	1,293.08	8.68
4	P4	2,384.94	4.71
5	P5	787.79	14.25
6	P6	743.57	15.10
7	P7	1,101.67	10.19
8	P8	939.75	11.95
9	P9	1,627.31	6.90

parapet walls, and thereby a precise determination of the rooftop rainwater harvesting potential by the stakeholder. Although the battery life of UAVs seems to be a limitation to cover very large areas, it is possible to cover larger extents by using multiple batteries or connected drone swarms. Furthermore, different types of UAVs can be used based on the extent of study area. Using fixed wing or hybrid UAVs enables the users to cover areas as large as a city. Recent studies by Hill & Rowan (2022), Shao *et al.* (2021), and Pfeifer *et al.* (2019) are a few examples where fixed wing drones were adopted to demonstrate their potentials in covering large areas. For instance, the study by Shao *et al.* (2021) covered about 158 km^2 using UAVs. Selecting UAVs that are compatible with advanced mission planning software can further minimize human efforts. However, it is advisable to continuously monitor the UAV flight. Eventually, the estimates derived

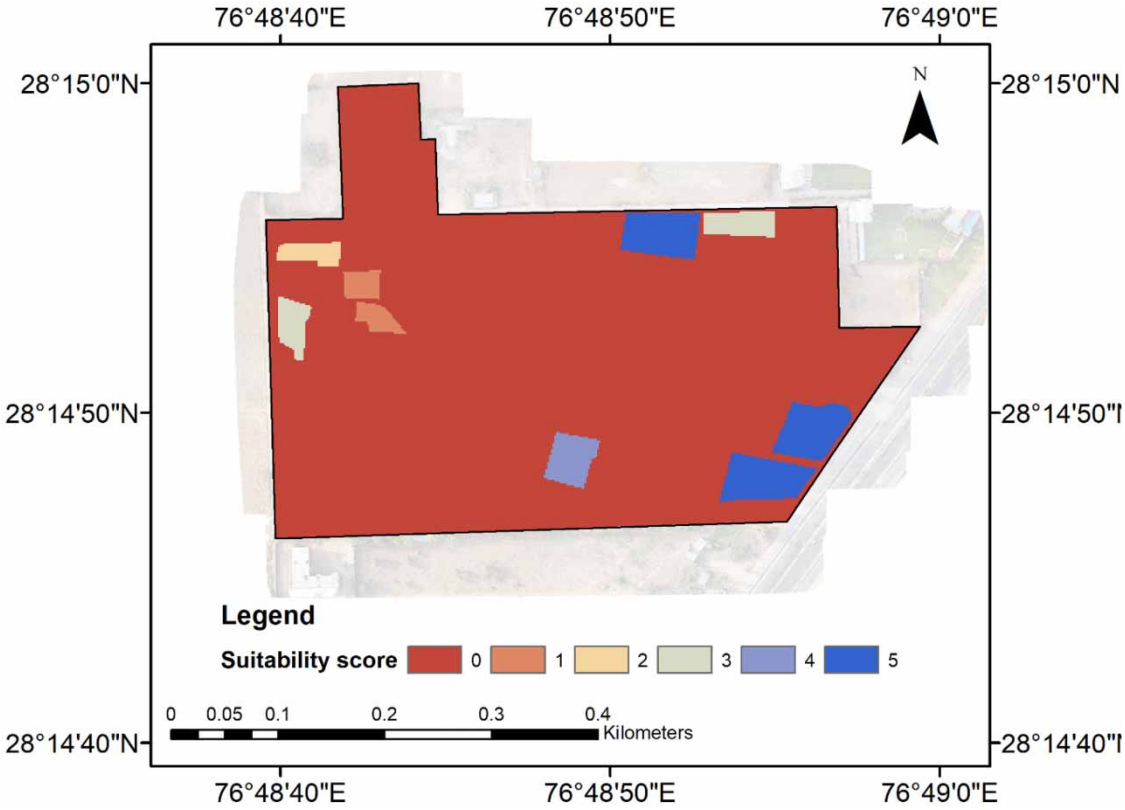

Figure 11 | Score based on excavation depth required to install the RWHS.

from the high-resolution datasets help in designing a new RWHS for a building and in determining the collection efficiency of the existing RWHS.

The present framework can be improved further to overcome a few challenges encountered in this study. For example, this study delineated the rooftops manually and then digitized these to generate a spatial database. The database finally helped compute the available rooftop area. This process enabled the researchers to visually inspect each building and thereby achieve a higher precision of classification. However, the implementation of this strategy on a community scale would be time-consuming. In this regard, the selection of an effective approach that minimizes manual classification while ensuring precision is imperative. Furthermore, the payload used in this study is an RGB camera that permits the user to capture the study site only in specific bands of the visible spectrum. Replacing this payload with a multi-spectral camera can further increase classification accuracy, particularly when automatic and semi-automatic classification techniques are adopted (Liu & Zhu 2020). The performance of object-based classification is observed to be superior to that of the pixel-based technique (Sibaruddin *et al.* 2018). Further research on object-based classification in the context of UAV imagery (high spatial resolution) may help attain a higher accuracy with the least human intervention. In addition to the computation of rooftop area using the drone imagery, combining the database obtained from drone surveys with data from weather forecasts, soil moisture sensors, and groundwater level measurements, water managers can make more informed decisions about water conservation and management. Drones can also be used to create detailed maps of RWHSs, including topography, soil types, and other features that can affect water management. This information can be used to design more efficient and effective systems. Performing a drone survey using the proposed framework can also help to determine the efficiency of an existing RWHS.

CONCLUSIONS

This study used a high-resolution orthomosaic developed using the UAV-generated imagery to delineate the rooftops in the study area and compute the available rooftop area to harvest rainwater. In addition, the generated orthomosaic helped in

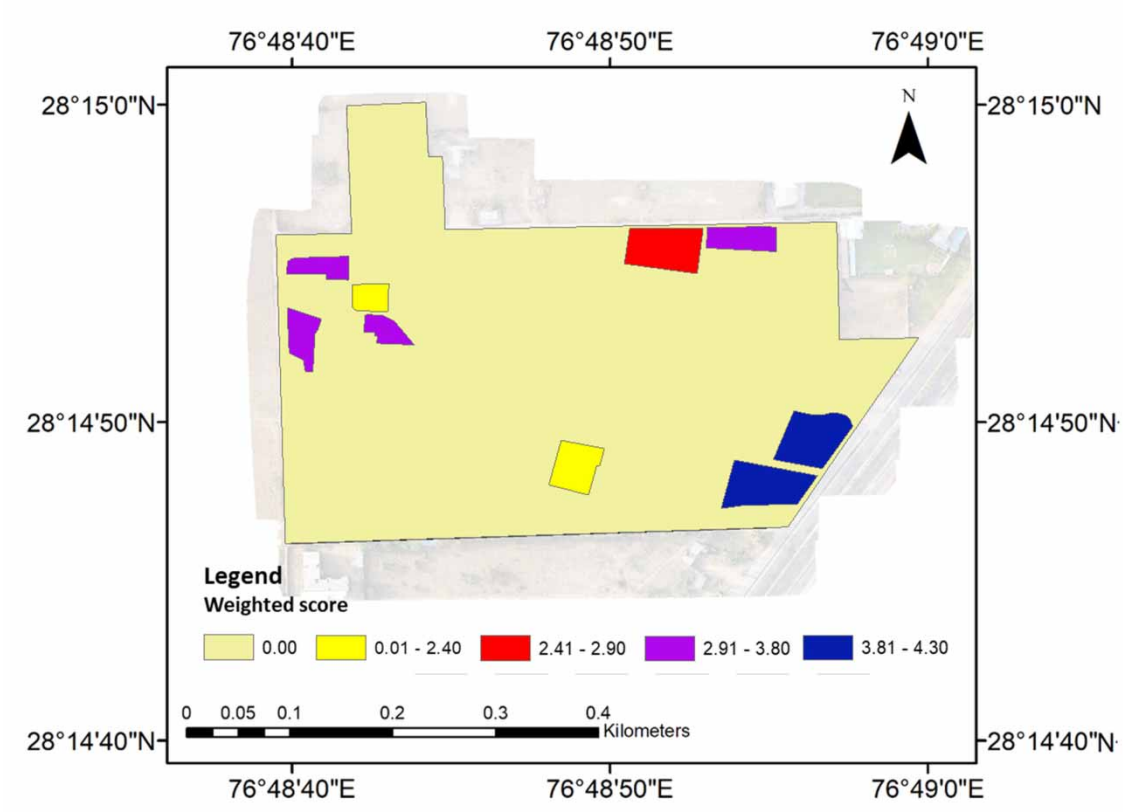

Figure 12 | Weighted score of each prospective site.

identifying the rooftop material. This enabled the determination of the attributes required to compute harvestable rainwater. The observations of the study affirm that the total rooftop area available for harvesting rainwater is 28,280.88 m^2. Out of this, 82.78% is concrete surface, and the remaining 17.22% is corrugated metal sheet roof. According to the material type, available area, and the average rainfall received in the study site, the total amount of water that can be harvested is 11,229 m^3. Note that the total harvestable water quantity was estimated using the coefficient derived from the Indian standard code book IS 15797 (2008). However, since the coefficients are expected to slightly differ with various characteristics of rooftops such as age and surface coating, a future study to determine these coefficients may further improve the precision of estimates. In addition, the WOT is used to identify the location suitable for constructing the storage tank. Two criteria are considered for the overlay analysis: the suitability for future expansion and the excavation required. Observations indicate that the site lying in the southeast of the study area is the most appropriate location for constructing the storage tank.

The outcomes of this study are twofold. First, the framework adopted demonstrates the capabilities of UAVs in acquiring high-resolution imagery, which can help conduct assessments of various parameters such as rooftop solar potential and green roof development potential. Second, the determination of the amount of harvestable water would generate a positive outlook, particularly in the context of the unprecedented rate of depletion of groundwater resources. It should be noted that the study estimated the quantity of harvestable rainwater by considering the average rainfall computed based on data of the past 30 years. Considering climate change, an optimal design can be achieved if machine learning models are employed to forecast future rainfall events by considering the historical rainfall data. The approach used in this study can also be adopted in proposing the RWHS at a community level, particularly in rural areas experiencing inadequate access to drinking water.

ACKNOWLEDGEMENTS

The authors acknowledge the support provided by the National Research Foundation of Korea (NRF) grant for the Brain Pool project (2021H1D3A2A02044785). Authors thank the ACIC-BMU foundation for providing the UAV to conduct the survey.

DATA AVAILABILITY STATEMENT

All relevant data are included in the paper or its Supplementary Information.

CONFLICT OF INTEREST

The authors declare there is no conflict.

REFERENCES

Aguiar, F. C., Bentz, J., Silva, J. M., Fonseca, A. L., Swart, R., Santos, F. D. & Penha-Lopes, G. 2018 Adaptation to climate change at local level in Europe: an overview. *Environmental Science & Policy* **86**, 38–63.

Angelakis, A. N. & Spyridakis, S. V. 1996 The status of water resources in Minoan times: a preliminary study. In: Angelakis, A.N., Issar, A.S. (eds) *Diachronic Climatic Impacts on Water Resources*. NATO ASI Series, vol 36, Springer, Berlin, Heidelberg, Germany, pp. 161–191.

Angelakis, A. N. & Koutsoyiannis, D. 2003 Urban water engineering and management in ancient Greek times. In:Stewart, B. A. and Howell, T. (eds). *The Encyclopedia of Water Science*. Dekker, New York, NY, USA, pp. 999–1007.

CGWB 2021 *Ground Water Year Book*. Central Ground Water Board, Haryana, India. Available from: http://cgwb.gov.in/Regions/NWR/Reports/GWYB%202020-21%20Haryana.pdf (accessed 25 July 2022).

Che-Ani, A. I., Shaari, N., Sairi, A., Zain, M. F. M. & Tahir, M. M. 2009 Rainwater harvesting as an alternative water supply in the future. *European Journal of Scientific Research* **34** (1), 132–140.

CPWD 2002 *Rainwater Harvesting and Conservation Manual*. Consultancy services organization, Central Public Works Department, Government of India, New Delhi, India.

FAO 2022. Available from: https://www.fao.org/home/en/ (accessed 15 October 2022).

Grajfoner, B., Butyrin, A. & Perc, M. N. 2017 Rainwater harvesting and green area retention potential detection using commercial unmanned aerial vehicles. *IOP Conference Series: Earth and Environmental Science* **90** (1), 012113. IOP Publishing.

Grunwald, L., Heusinger, J. & Weber, S. 2017 A GIS-based mapping methodology of urban green roof ecosystem services applied to a central European city. *Urban Forestry & Urban Greening* **22**, 54–63.

Hill, A. C. & Rowan, Y. M. 2022 The black desert drone survey: new perspectives on an ancient landscape. *Remote Sensing* **14** (3), 702.

Huang, R., Dong, L. & Wu, L. M. 2015 Status analysis of Chengdu city green roof based on GIS. *Chinese Landscape Architecture* **31** (01), 79–82.

IS 15797: 2008 (Indian Standard) 2008 *Roof top Rainwater Harvesting Guidelines*. Bureau of Indian standards, New Delhi, pp. 1–14.

Kakoulas, D. A., Golfinopoulos, S. K., Koumparou, D. & Alexakis, D. E. 2022 The effectiveness of rainwater harvesting infrastructure in a Mediterranean island. *Water* **14** (5), 716.

Karteris, M., Theodoridou, I., Mallinis, G., Tsiros, E. & Karteris, A. 2016 Towards a green sustainable strategy for Mediterranean cities: assessing the benefits of large-scale green roofs implementation in Thessaloniki, Northern Greece, using environmental modelling, GIS and very high spatial resolution remote sensing data. *Renewable and Sustainable Energy Reviews* **58**, 510–525.

Liu, S. & Zhu, H. 2020 Object-oriented land use classification based on ultra-high resolution images taken by unmanned aerial vehicle. *Transactions of the Chinese Society of Agricultural Engineering* **36**, 87–94.

Melese, T. & Belay, T. 2022 Groundwater potential zone mapping using analytical hierarchy process and GIS in Muga Watershed, Abay Basin, Ethiopia. *Global Challenges* **6** (1), 2100068.

Pala, G. K., Pathivada, A. P., Velugoti, S. J. H., Yerramsetti, C. & Veeranki, S. 2021 Rainwater harvesting-A review on conservation, creation & cost-effectiveness. *Materials Today: Proceedings* **45**, 6567–6571.

Peddinti, P. R. T. & Kim, B. 2022 Efficient pavement monitoring for south korea using unmanned aerial vehicles. In: *International Conference on Transportation and Development 2022*. ASCE, pp. 61–72. https://doi.org/10.1061/9780784484357.006.

Pfeifer, C., Barbosa, A., Mustafa, O., Peter, H. U., Rümmler, M. C. & Brenning, A. 2019 Using fixed-wing UAV for detecting and mapping the distribution and abundance of penguins on the South Shetlands Islands, Antarctica. *Drones* **3** (2), 39.

Puppala, H. & Singh, A. P. 2021 Analysis of urban heat island effect in Visakhapatnam, India, using multi-temporal satellite imagery: causes and possible remedies. *Environment, Development and Sustainability* **23** (8), 11475–11493.

Radonic, L. 2019 Re-conceptualising water conservation: rainwater harvesting in the desert of the southwestern United States. *Water Alternatives* **12** (2), 699–714.

Shao, H., Song, P., Mu, B., Tian, G., Chen, Q., He, R. & Kim, G. 2021 Assessing city-scale green roof development potential using Unmanned Aerial Vehicle (UAV) imagery. *Urban Forestry & Urban Greening* **57**, 126954.

Sharma, A. & Begbie, D. 2015 *Rainwater Tank Systems for Urban Water Supply: Design, Yield, Energy, Health Risks, Economics and Social Perceptions*. IWA Publishing, London, UK.

Sibaruddin, H. I., Shafri, H. Z. M., Pradhan, B. & Haron, N. A. 2018 Comparison of pixel-based and object-based image classification techniques in extracting information from UAV imagery data. *IOP Conference Series: Earth and Environmental Science* **169** (1), 012098. IOP Publishing.

Tian, Y. & Jim, C. Y. 2011 Factors influencing the spatial pattern of sky gardens in the compact city of Hong Kong. *Landscape and Urban Planning* **101** (4), 299–309.

Ward, S., Memon, F. A. & Butler, D. 2010 Harvested rainwater quality: the importance of appropriate design. *Water Science and Technology* **61** (7), 1707–1714.
Ward, S., Memon, F. A. & Butler, D. 2012 Performance of a large building rainwater harvesting system. *Water Research* **46** (16), 5127–5134.
Zhou, D., Liu, Y., Hu, S., Hu, D., Neto, S. & Zhang, Y. 2019 Assessing the hydrological behaviour of large-scale potential green roofs retrofitting scenarios in Beijing. *Urban Forestry & Urban Greening* **40**, 105–113.

First received 27 December 2022; accepted in revised form 14 April 2023. Available online 27 April 2023